Volume 81 (2023) 01-14

boletim paranaense de Geociências
ISSN: 0067-964X

STRESS CORROSION CRACKING FAILURE OF INLAND 303 STAINLESS STEEL ANCHOR BOLT: BOLT AND ROCK CHARACTERISTICS INFLUENCE

DOUGLAS JOÃO FILIPAK[1], IRIVAN GUSTAVO BURDA[1], EUCLIDES ALEXANDRE BERNARDELLI[1], ALESSANDRA DE BARROS E SILVA BONGIOLO[2], PEDRO CUNHA DE LIMA[3], YURI MARTINS CAMPOS[3]

1 - Universidade Tecnológica Federal do Paraná - UTFPR. Av. Sete de Setembro, 3165 - Rebouças, 80230-901 - Curitiba - PR - Brasil. E-mail: douglasfilipack@gmail.com; piramundo@gmail.com; ebernardelli@utfpr.edu.br

2 - Universidade Federal do Paraná - UFPR. Avenida Coronel Francisco H. dos Santos, 100 - Jardim das Américas, 81530-000 - Curitiba - PR - Brasil. E-mail: alebongiolo@gmail.com

3 - Instituto Federal da Bahia - IFBA. R. Emídio dos Santos, s/n - Barbalho, 40301-015 - Salvador - BA - Brasil. E-mail: pedrolima@ifba.edu.br; yuricampos@ifba.edu.br

Abstract *- A serious climbing accident in the Brazilian city of Itatim - BA was caused by the rupture of four anchor bolts after the athlete stopped at an anchor point to rest. Bolt fracture characteristics suggest failure by stress corrosion cracking (SCC), however the great distance from major sources of aggressive agents and the low age of the anchor bolt are concerning. The objective of the work is to evaluate the failure causes focusing specifically on rock and bolt characteristics. Laboratorial results indicate typical composition of a 303 SS, rich in MnS, high levels of residual stress from manufacture and relevant concentrations of Chloride along the bolt cracks. Rock analysis shows no aggressive component in its composition. The investigation concluded that high ion concentrated water inside the hole, along with low corrosion resistance of the bolt material, 303 SS, and manufacturing residual stress were the main factors that contributed for the SCC failure. No evidence that supports the influence of the rock characteristics was found.*

Keywords: *Inselberg; Stress corrosion cracking (SCC); Manganese sulfide; 303 stainless steel; anchor bolt;*

boletim paranaense de Geociências
ISSN: 0067-964X

1. INTRODUCTION

In April 2023 a serious climbing accident occurred in Itatim-BA, Brazil. The region is well known in the climbing community for its inselberg, gneissic, and granitic formations that rise isolated over plains. Itatim accommodates 30 sectors with more than 500 climbing routes. The accident occurred after four anchor bolts, designed for a shear load of 28 kN each, broke under a presumable nearly static load off less than than 1kN. The climber fell 10m directly to the ground after hanging from a quickdraw for rest. Days later, on the same route, some bolts were tested for shear, under just body weight, and for torsion, with a hand wrench, and broke, raising the possibility that the entire route could be compromised. No other anchor bolt in the region showed the same kind of failure. The bolts were oxidized, and a brittle fracture was observed in the most corroded region.

This type of fracture was already reported before and indicates a relationship with stress corrosion cracking (SCC) in stainless steel bolts. UIAA Safety Commission (2020) describes the relationship between seashore locations and SCC. As Itatim is located inland, far from the sea or industries, natural corrosive agents, such as rock components, could have caused the failure. The Bolt age is also an concern, as the installation was made less than 10 years before. The objective of the present work is to evaluate the main causes of the bolt failure and trace its relationship with rock and bolt characteristics.

Figure 1 - Failed anchor bolt analyzed, Sample

2. GEOLOGY OF ITATIM

The geology of Itatim, located in the state of Bahia, Brazil, is notable for its complexity and richness in terms of rock formations and mineral resources. This region, situated in the north-central part of Bahia, is known for its impressive inselberg landscapes, which are residual reliefs mainly composed of granitic and gneissic rocks.

Itatim is part of the São Francisco Craton, one of the oldest geological units in Brazil, dating back to the Archean and Paleoproterozoic eras. The local geology is dominated by crystalline rocks that are part of the Gneiss-Migmatite Complex, a set of high-grade metamorphic rocks primarily consisting of gneisses, migmatites, granites, and amphibolites. Studies have revealed a complex interaction of tectonic events that have shaped the landscape over geological time (Almeida & Hasui, 1984).

Gneissic rocks predominate in the region, characterized by their banded texture and varied mineralogical composition, including quartz, feldspar, biotite, and occasionally garnet (Pedreira & de Brito Neves, 2005). Migmatites are hybrid rocks resulting from the partial melting of pre-existing rocks, presenting leucosome (melted part) and melanosome (refractory part) structures (Oliveira et al., 2010).

boletim paranaense de Geociências
ISSN: 0067-964X

Granite bodies are common and hold great economic importance due to their use as construction material. These granites are generally medium to coarse-grained, composed of quartz, feldspars (mainly orthoclase and plagioclase), and micas (Pedreira & de Brito Neves, 2005).

Less abundant, amphibolites are high-grade metamorphic rocks composed predominantly of amphiboles and plagioclase feldspars, indicating a geological environment that has been subjected to high pressure and temperature conditions (Pedreira & de Brito Neves, 2005).

The Itatim region is marked by a series of geological structures that highlight the area's tectonic complexity. Folds, faults, and fractures are common, indicating a history of intense tectonic events (Silva & Fuck, 2010). Inselbergs, residual geological formations that stand out in the landscape, are the result of differential weathering and erosion of more resistant rocks (Oliveira et al., 2010).

The inselbergs of Itatim are one of the most distinctive aspects of the local geomorphology. These isolated elevations are formed by rocks resistant to erosion, such as granites and gneisses, which stand out amid a flatter relief. The region's geomorphology is influenced by physical and chemical weathering processes that act on the decomposition and disintegration of rocks (Oliveira et al., 2010).

3. MATERIALS AND METHODS

For the characterization of the rock, samples were collected and sent for petrographic analyses: macroscopic analysis complemented by microscopic analysis of thin sections using transmitted light. Equipment: Carl Zeiss petrographic microscope, model AXIO Imager.A2m. Image capture and processing system AxioVision.

Two bolts were taken from the climbing route, identified here as Sample A and Sample B. For sample B, bolt and nut were analyzed. They were sectioned into the region of the fracture and submitted to optical microscopy to preliminary determine material properties, such as grain size, material type, inclusions, and fracture pattern. Scanning Electron Microscopy (SEM) provided extra magnification and helped in the analysis of the fracture, crack, and inclusions. For a more precise composition analysis sample A was submitted to Energy-Dispersive X-Ray Spectroscopy (EDS) that provided a semi-quantitative percentual composition of the material, although results may exhibit especially high percentual errors for lighter elements, such as Carbon (C) and Oxygen (O). As the methods previously mentioned could not inform martensite presence in the samples, sample B was submitted to X-ray diffractometry (XRD), that can identify martensite, austenite, and ferrite phases in the steel. As hardness can play an important role in SCC, hardness tests were conducted via Vickers microhardness.

In addition to the pair of failed samples analyzed, two brand new bolts were analyzed with a similar methodology. One AISI 304 steel bolt and one AISI 316L bolt. These control samples were chosen due to their established reputation and reliability, since a brand related problem could be possible. One sample of rock surface was collected. Internal and external surfaces were analyzed for chemical composition, primarily, via EDS, and for a more reliable and precise composition and characterization, a Petrographic Macroscopy and Transmitted Light Microscopy were conducted.

4. RESULTS

According to the descriptions provided by the Laboratório de Análise de Minerais e Rochas (iLAMIR/UFPR), the rock sample taken from the accident site was characterized as an

boletim paranaense de Geociências
ISSN: 0067-964X

igneous rock, dark gray in color, with fine to medium grain size, massive structure, and fine to medium phaneritic inequigranular texture. Regarding its alteration state, it was classified as: Fresh rock in terms of weathering, but showing incipient hydrothermal alteration.

The microscopic characteristics observed allowed the rock sample to be classified as a Monzogranite with fine to medium phaneritic inequigranular texture and massive structure. It is composed of quartz, alkali feldspar (microcline), plagioclase (oligoclase), biotite, and opaque minerals. As secondary minerals, sericite, carbonate, and chlorite occur, being products of hydrothermal alteration. The hydrothermal alteration is incipient, non-pervasive, and occurs restricted to a few crystals. Macroscopic and microscopic photographs, percentages of the minerals in the rock, and descriptions of each mineral can be verified in the analysis certificate number 2023 095 petro, in Appendix A of this manuscript.
Optical microscopy realized in Sample A could not reveal grain boundary, although crack formation and a high density of precipitates can be observed in Figures 2 and 3. Electron microscopy of Sample A and Sample B revealed more details of the microstructure and crack formation.

Figure 3 displays the propagation of primary and secondary cracks in sample A via optical microscopy, with clear signs of corrosion. Figures 3 and 4 indicate oxidation preference by twinned regions and clusters of precipitates, with inter and intra granular propagation in both Sample A and the bolt of Sample B, respectively. Cracks were found via SEM in the nut of sample B.

In the longitudinal section these precipitates present an elongated configuration, and it can be seen in Figure 6 that they are crack initiation points, although cracks don't follow them in the longitudinal direction.

SEM images of the fracture in Sample A are displayed in Figures 7 and 8. The images magnified at 500x reveal the various micro cracks, evincing great embrittlement.

Twins can be seen in both SEM and Optical microscopy images. Martensite presence was confirmed in Sample B via XRD. Martensite appears in Figure 5 as α' peaks, while Austenite in γ peaks.

Table 1 shows the mean composition obtained by EDS at different regions of sample A and the mean values for the 304 and 316L samples, in comparison with standard composition for AISI 304, AISI 316 and AISI 303 SS. Matrix composition for Sample A approximates the expected for AISI 304 SS. Precipitates, in other hand, show high values of Manganese (Mn), Sulfur (S), and copper (Cu). Nickel values were found to be 7%-10% lower than expected in every sample.

Section cracks composition varies considerably from those of the Matrix and Precipitates. Sodium (Na) and Chlorine (Cl) appear in the form of oxides, as well as small values of Sulfur (S) and Potassium (K). In the fracture surface, oxide presence is much larger in comparison with other regions, with Sodium (Na) and Chlorine (Cl) as the main components, and Potassium (K) in similar amount as found in the cracks.

Table 2 shows the results of hardness profile via Vicker testing. In the test, sample A presented stable values spatially. Selecting measures by microstructure, in sample B, showed a variation of 10% between twined and non-twinned grains. 304 and 316L anchor bolts showed values of hardness around 60% smaller when compared to the mean found in Sample A and B.

boletim paranaense de Geociências
ISSN: 0067-964X

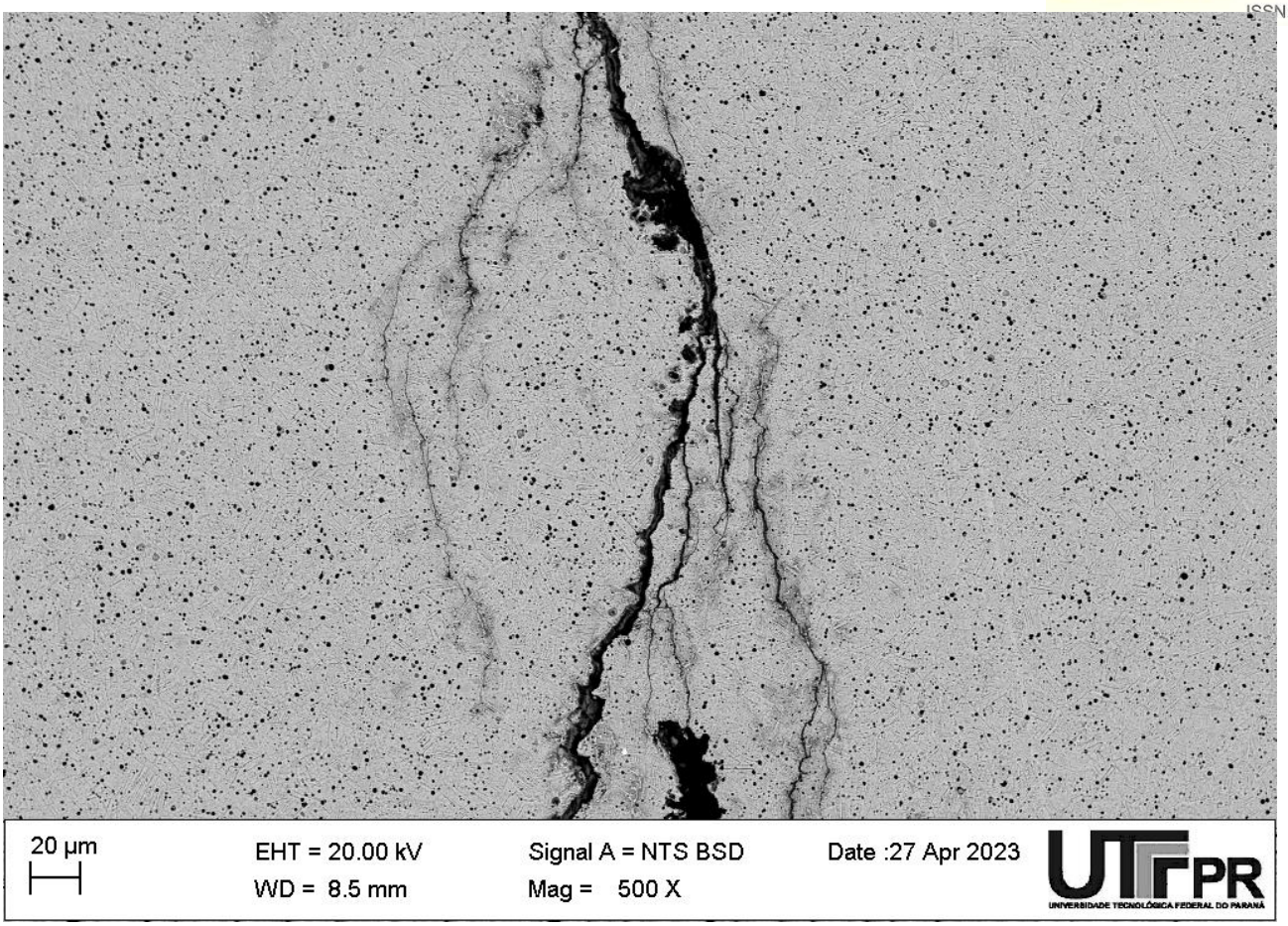

Figure 2 - Main crack on the section and derivations, Sample A, failed bolt, SEM**.**

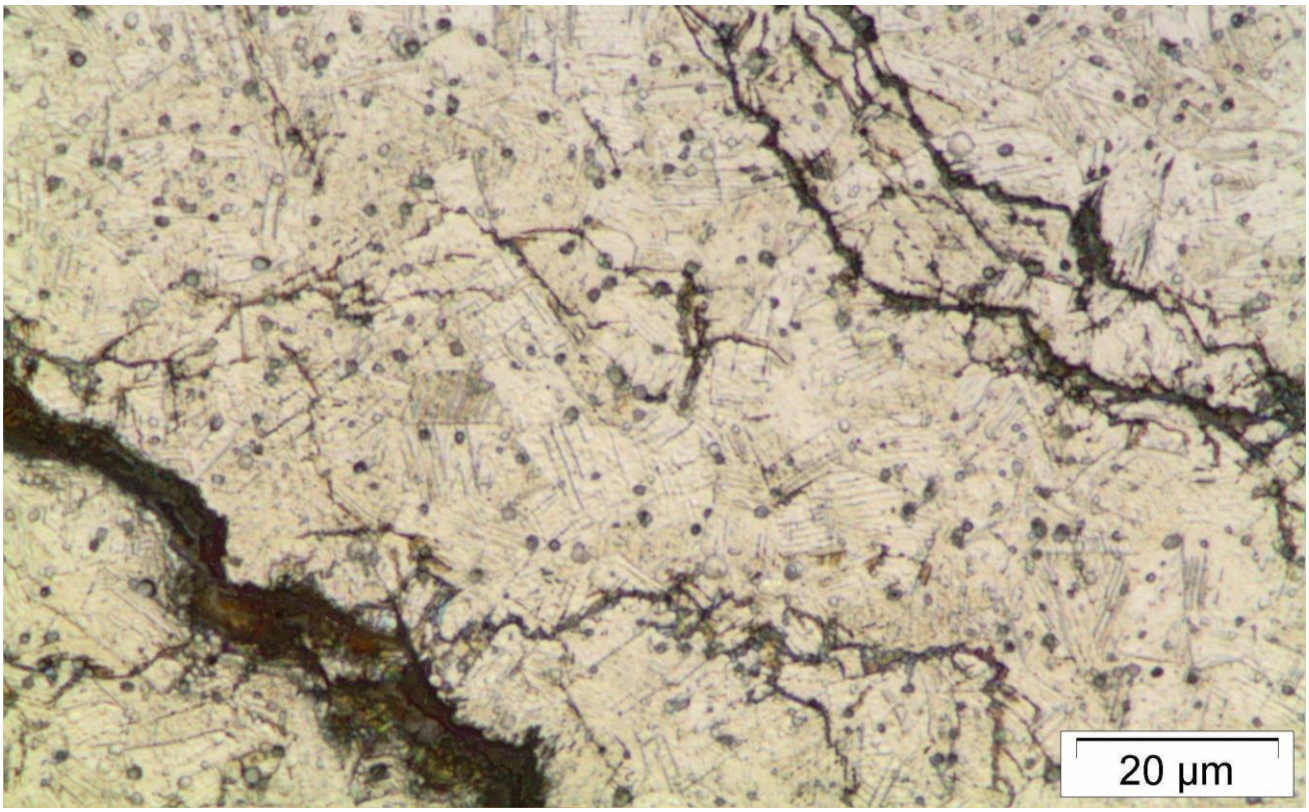

Figure 3 - Main crack on the section and derivations, Sample A, failed bolt, transversal section, Optical Microscope

boletim paranaense de Geociências
ISSN: 0067-864X

Region	C	O	Na	Si	S	Cl	K	Ca	Cr	Mn	Fe	Ni	Cu	Mo
Matrix (Sample A)	9,93	0,52	0,00	0,65	0,00	0,00	0,00	0,00	16,82	1,33	62,78	7,21	0,66	0,00
Precipites (Sample A)	11,66	1,43	0,00	0,35	7,17	0,00	0,00	0,10	13,89	12,02	44,98	4,60	3,78	0,00
Cracks (Sample A)	0,00	39,16	5,59	0,62	0,82	1,27	0,34	0,24	13,86	0,85	33,97	2,63	0,38	0,00
Fracture Black Oxides (Sample A)	0,00	53,95	39,22	0,44	0,00	0,11	0,13	0,00	1,25	0,26	3,84	0,80	0,00	0,00
Fracture Gray Oxides (Sample A)	0,00	39,29	2,02	0,05	0,04	1,97	0,34	0,00	3,34	0,60	45,34	6,99	0,00	0,00
304 (Control sample)	5,45	1,79	0	0,46	0	0	0	0	18,11	0,9	64,7	7,4	1,5	0,00
316L (Control sample)	5,50	0,00	0,00	0,53	0,00	0,00	0,00	0,00	16,44	1,15	65,22	9,19	0,00	1,98
AISI 303 Standard	0,15	-	-	<1,0	>0,15	-	-	-	17,0 – 19,0	<2,00	-	8,0 – 10,0	-	-
AISI 304 Standard	0,08	-	-	<1,0	<0,03	-	-	-	18,0 – 20	<2,00	-	8,0 – 11,0	-	-
AISI 316 Standard	0.08	-	-	<1,0	<0,03	-	-	-	16,0 – 18,0	<2,00	-	10,0 – 14,0	-	2,0 – 3,0

Table 1 - Main values of element composition evaluated by EDS divided by interest region, sample and Standard values.

boletim paranaense de Geociências
ISSN: 0067-964X

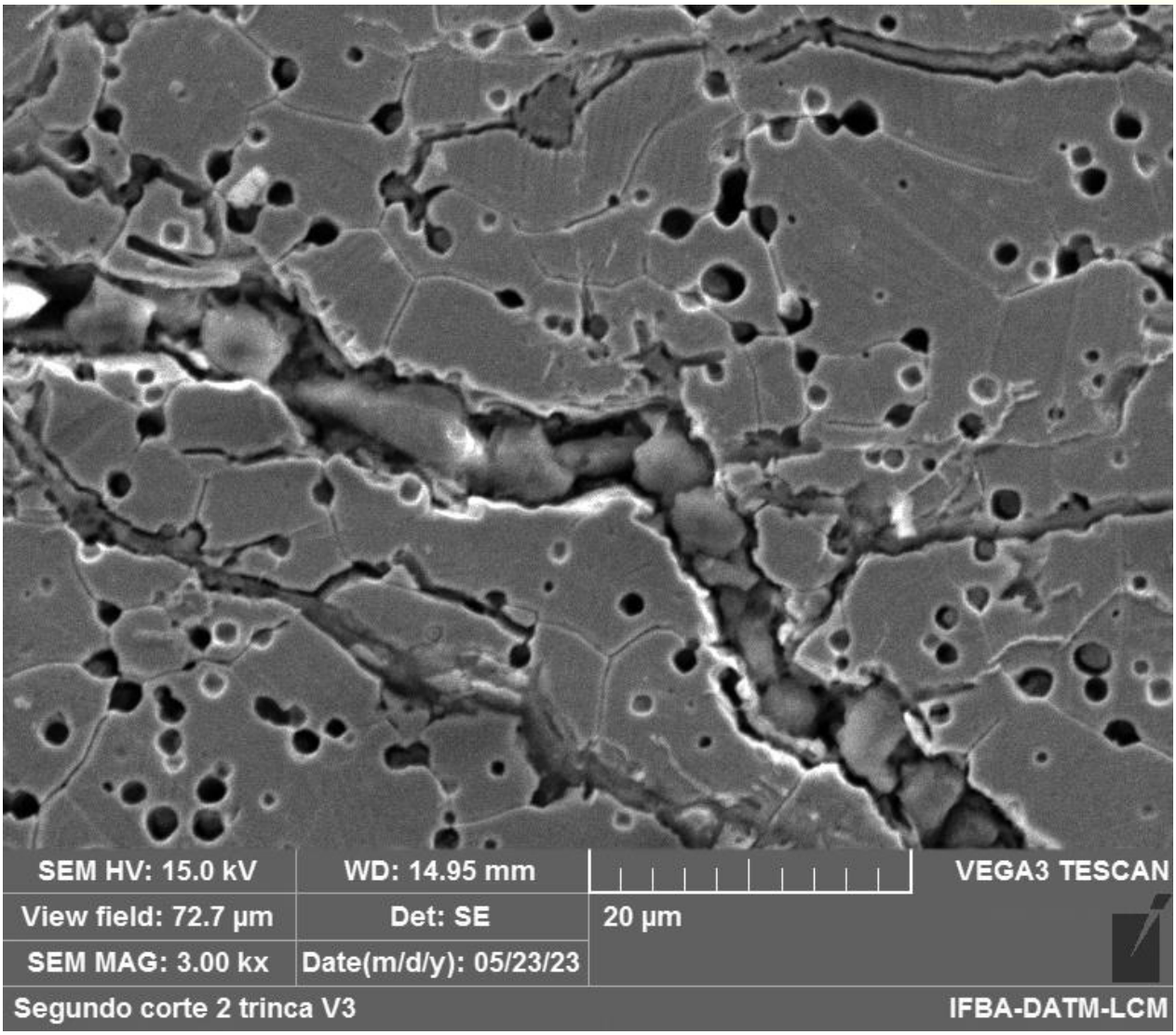

Figure 4 - Propagation of main and secondary cracks, failed bolt, Sample B, transversal section, SEM.

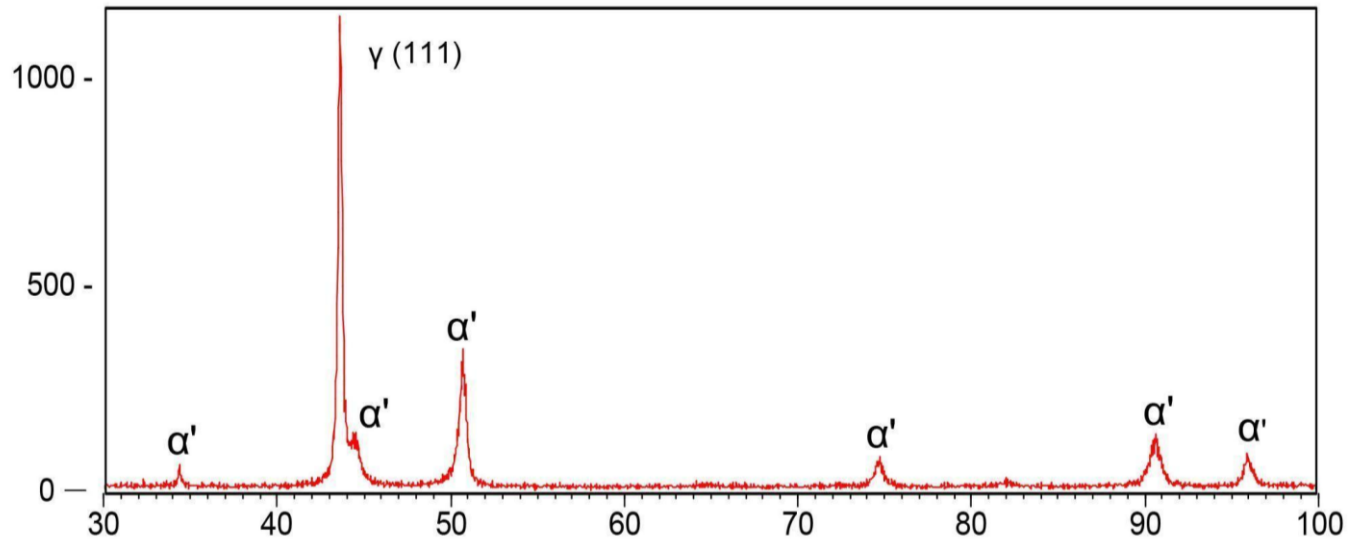

Figure 5 - XRD results shows Austenite presence (γ) and martensite (α').

boletim paranaense de Geociências
ISSN: 0067-964X

Sample	Distance from edge (mm)	Microstructure	Mean Hardness	Standard Deviation	General Mean
A	0,01	-	314	51	305 ±22
	1	-	314	5	
	2	-	306	6	
	3	-	298	14	
	4	-	292	4	
B	-	Twined	305	3	292 ±16
	-	Untwined	277	8	
304 (control sample)	0,01	-	167	5	165 ±12
	1	-	175	11	
	2	-	156	14	
	3	-	175	4	
	4	-	158	1	
	5		160	2	
316L (control sample)	0,01	-	171	3	176 ±14
	1	-	197	3	
	2	-	163	12	
	3	-	176	1	
	4	-	163	1	
	5	-	186	8	

Table 2 - Vickers hardness profile in various samples and regions.

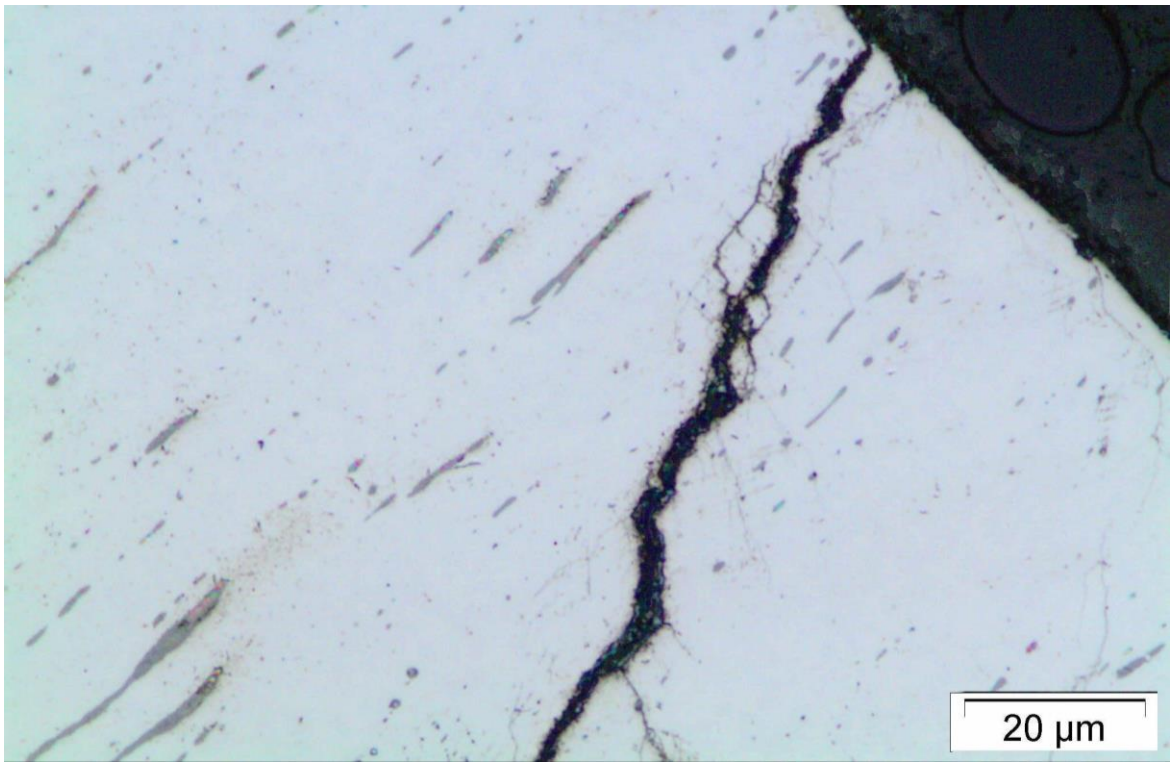

Figure 6 - Propagation of a crack and MnS precipitates in the longitudinal section of sample A, longitudinal section, SEM.

boletim paranaense de Geociências
ISSN: 0067-964X

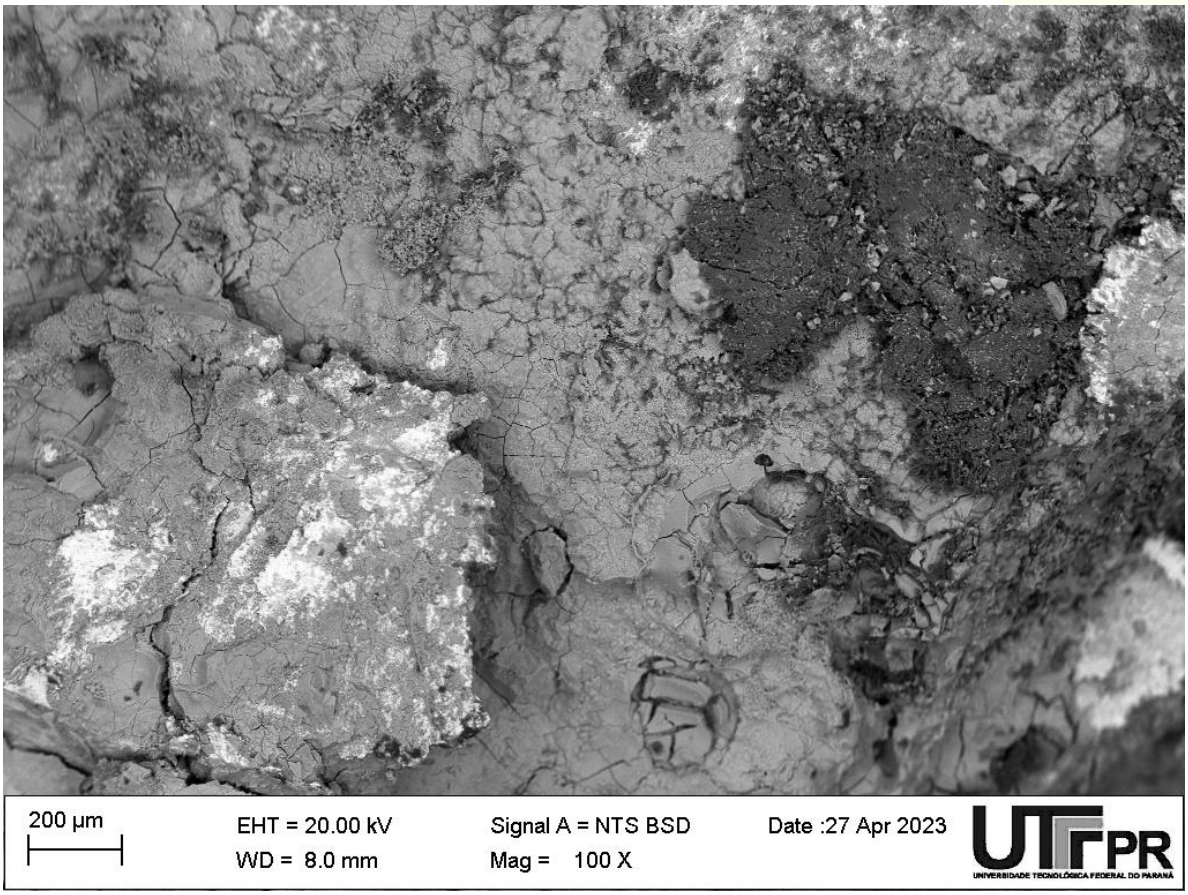

Figure 7 - Fracture image, darker regions show oxide crystals formation, SEM.

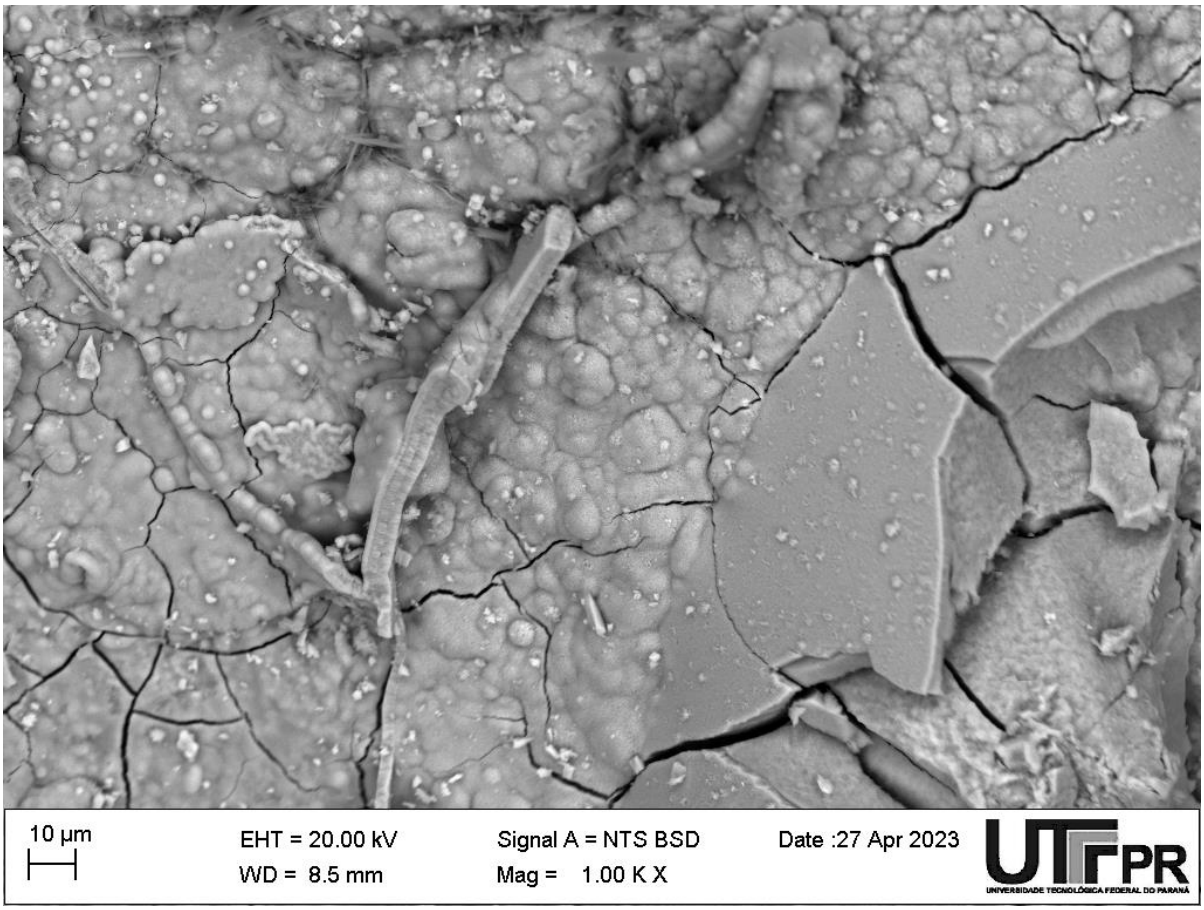

Figure 8 - Cracks on the fractured surface, including a fractured MnS, SEM.

5. DISCUSSIONS

boletim paranaense de Geociências
ISSN: 0067-964X

Stress corrosion cracking may be considered the main cause of failure. Cracks can be seen in both Sample A and B, in sample A they are as large as half of the bolt section. Corrosion products confirm that the cracks are a result of the combination of stress and corrosion, and not of only mechanical stress. Fracture images also show high embrittlement. Raja & Tetsuo (2011) review summarizes these aspects as typical in SCC failure based on diverse sources. Still accordingly to the report, austenitic stainless steels, AISI 300s series, are prone to SCC in high electrolyte concentrate aqueous medium, such as marine environment, in temperatures above 50°C-60°C. But some other factors may increase susceptibility to SCC, such as material composition, treatment and precipitate formation, residual stress and other environmental factors, as is discussed below.

Considering the composition of the matrix and the high concentration of Manganse (Mn) and Sulfur (S) rich precipitates, the material was identified as AISI 303 SS, in which Sulfur (S) is added in steel manufacture to form Manganese Sulfide (MnS)., (International Organization for Standardization, 2014). Copper (Cu) was also found in high concentrations near the precipitates, and its affinity with MnS is known (Lillard, Ka, Marjan & Niu, Wei, 2016). Microstructure appearance in the longitudinal section is typical of rolled AISI 303 SS, (Newby, Mills & Asm Handbook Committee, 1985). MnS is known for contributing to corrosion because: it destabilizes the passive layer, serving as an initiation point of oxidation, as the weaker passive layers breaks and water makes contact with the Iron (Fe) matrix (Duan, Man, Cui, Hong-Zhi, et al, 2022; Muto, Izumiyama, & Hara, 2007); the region around it has a higher anodic potential, that is translated in a lower oxidation resistance area and a preferential corrosion path (Suter & Bohni, 2001; Vuillemin, Philippe, et al, 2003); its dissolution produces H+, which makes the medium more aggressive, especially around the MnS inclusions (Alnajjar, Christien, Barnier, Bosch, Wolski, Fortes & Telling, 2020); finally, it serves as tension concentrator points, for crack propagation, leading the corrosion through specially prone areas (Gu, Lian, Bao, Xiao, & Muenstermann, 2019). Figure 10 offers a visual schema of how MnS promotes corrosion and crack propagation.

Besides material composition, manufacture methods could have contributed for the bolt susceptibility to SCC. The formation of twins is evidence of cold work during manufacture, especially when associated with martensite formation, as found in Sample B (Ławrynowicz, Zdzisław, 2019), leading to residual stress, one of the factors that may reduce austenitic SS resistance to SCC, as mentioned above. The residual stress is confirmed in the microhardness profile, ans seen in Table 2, as the mean hardness found in Sample A and B are equivalent to a degree of cold work between 20%-30% in a 300 series stainless steel, (Milad, Zreiba, Elhalouani, & Baradai, 2008; Moen & Duncan, 1976). Ahile for 304 and 316 control samples, hardness was much lower, indicating lower levels of cold work, between 0% and 10%. These high levels of stress found in Sample A and Sample B offers critical conditions for SCC: the increase in MnS reactivity on the surface, helping in the initiation and progress of corrosion (Suter & Bohni, 2001); martensite induced due to cold work reduces the corrosion resistance of SS (Gauzzi, Montanari, Principi & Tata, 2006); and the stress necessary for the propagation of the crack, which is gradually opened and corroded. In experiments with a sodium chloride solution at high temperature, AISI 304 SS presents SCC starting with 10% of cold work, and 30% for steel AISI 316L, the results show that the corrosion speed increases exponentially with the degree of cold work, as showed by Cigada, Mazza, et al (1982).

The source of Clorine (Cl), Sodium (Na) and Potassium (K) could not be evaluated in this work, as the rock did not present any significant amount of these components, and none other main source can be hyphotized, such as sea salt or industry wastes. However, in Itatim, the rainfall regime is variable, with periods of heavy precipitation and periods of prolonged drought, with temperatures varying from 20°C to 30°C, according to Prefeitura municipal de Itatim (2020). UIAA Safety Commission (2021) has already warned about the lack of frequent washing of the piece by rain since salt concentration is more important than water volume in the case of corrosion. This is because

boletim paranaense de Geociências
ISSN: 0067-964X

the main mechanism of corrosion in a bolt inside a hole is crevice corrosion, in which oxygen concentration difference between the surface of the liquid and its bottom causes a pile that increases its strength through time by acidification, that facilitates electronic changes, and by oxygen consumption, that raises the difference in oxygenation and build up corrosion potential. Rain washing can mitigate this process by renewing water inside the hole, maintaining pH closer to neutral and oxygen differences constant. Figure 9 provides a visual representation of the process.

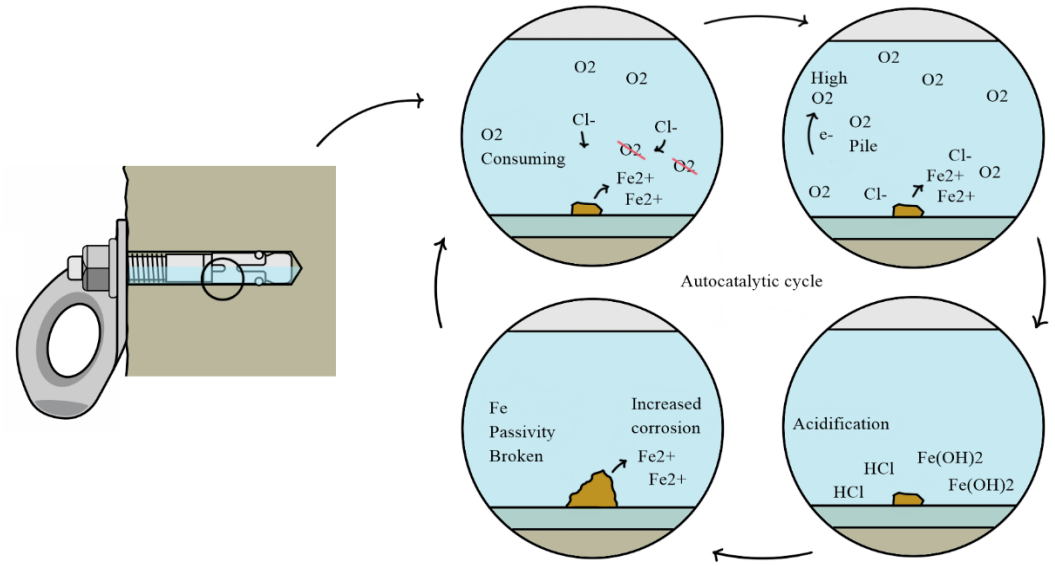

Figure 9 - Illustration of crevice corrosion mechanism in an anchor bolt hole. Source: Authors own elaboration.

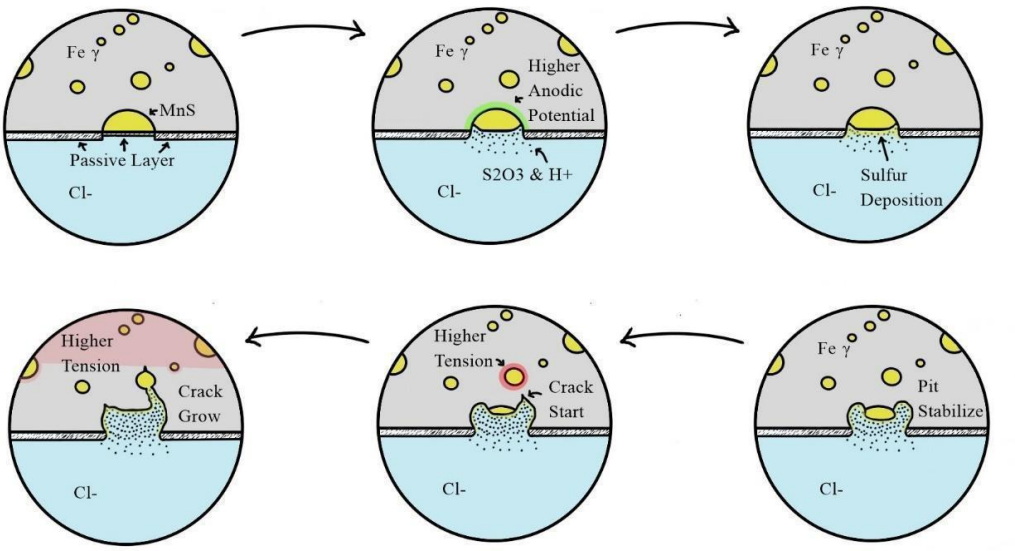

Figure 10 - Illustration of SCC facilitated by Mn. Source: Authors own elaboration

6. CONCLUSIONS

The results of the analysis presented in this article conclude that the failure in the material occurred by SCC mechanism in a rainwater filled hole, with elevated concentration of ions, being the composition of the bolt, made of 303 SS, the main contributor factor for reducing the bolt expected resistance for corrosion. There is no evidence that supports the influence of the rock characteristics in the mechanism nor any other environmental factor.

The results of the analysis presented in this article conclude that:

boletim paranaense de Geociências
ISSN: 0067-964X

1. The failure mechanism that led to the anchor failure was SCC initiated by crevice corrosion in a medium rich in chlorides, possibly pre-acidified, at a temperature substantially higher than that of the environment, facilitated by the composition of the material, rich in MnS.
2. The residual stress in the fractured anchor bolt is demonstrated by the elevated hardness and martensite presence, the result of high deformation during the manufacturing process without proper subsequent heat treatment being carried out. These stresses were sufficient for crack propagation, especially in conjunction with MnS.
3. After the cold work, some kind of stress relief and solubilization is recommended. For stainless steel alloys containing carbon, stress relief in higher temperatures with cooling by quenching prevents chromium carbide precipitation in temperature ranging from 425°C to 900 °C and maintains a moderate SCC resistance. For low carbon alloys, most high temperature stress reliefs are suitable for moderate SCC resistance. British stainless-steel association (2024) shows these and other recommendation for stress reliving in stainless steel.
4. For structural applications, especially in the case of personal safety equipment, sulphurated, non-stabilized and standard carbon stainless steel should be avoided. This work shows the impact of MnS in SCC resistance in 304 SS, while stabilized and low carbon alloys are known for its superior corrosion and sensitization resistance.
5. The lack of traceability on the part increases the difficulty of identifying the problem, as well as to carry out corrective measures and prevent further accidents. Even so, the effort to track routes that have been equipped with this anchor bolt model in the region can prevent new accidents.
6. The chloride found in the piece can be identified as NaCl. Presence of S in the rock could be from acid rain, but its origin is uncertain. The origin of these contaminants needs to be further investigated to understand the level of aggressivity of the environment in Itatim, as the presence of S and NaCl from natural or artificial sources may cause corrosion. As for any outdoor application it is hard to prevent moisture containing some kind of ions that induce corrosion, so the safest alloys must be selected to survive for a long time.
7. The presence of aggressive agents was not verified in the composition of the rock, but a deeper study may reveal more information.

7. REFERENCES

ALMEIDA, F. F. M.; HASUI, Y. O Pré-Cambriano do Brasil. São Paulo: Edgard Blücher, 1984.

ALNAJJAR, M.; CHRISTIEN, F.; BARNIER, V.; BOSCH, C.; WOLSKI, K.; FORTES, A.; TELLING, M. Influence of microstructure and manganese sulfides on corrosion resistance of selective laser melted 17-4 PH stainless steel in acidic chloride medium. Corrosion Science, v. 168, 108585, 2020. doi: 10.1016/j.corsci.2020.108585.

BRITISH STAINLESS STEEL ASSOCIATION. Stress Relieving Heat Treatments for Austenitic Stainless Steels. Disponível em: https://bssa.org.uk/bssa_articles/stress-relieving-heat-treatments-for-austenitic-stainless-steels/. Acesso em: 26 jul. 2024.

CIGADA, A.; MAZZA, B.; PEDEFERRI, P.; SALVAGO, G.; SINIGAGLIA, D.; ZANINI, G. Stress corrosion cracking of cold-worked austenitic stainless steels. Corrosion Science, v. 22, p. 559-578, 1982. doi: 10.1016/0010-938X(82)90055-5.

DUAN, Z.; MAN, C.; CUI, H.; ZHONGYU, C.; WANG, X. Formation mechanism of MnS inclusion during heat treatments and its influence on the pitting behavior of 316L stainless steel fabricated by laser powder bed fusion. Corrosion Communications, v. 7, 2022. doi: 10.1016/j.corcom.2022.04.002.

GAUZZI, F.; MONTANARI, R.; PRINCIPI, G.; TATA, M. AISI 304 steel: anomalous evolution of martensitic phase following heat treatments at 400°C. Materials Science and Engineering: A, v. 438-440, p. 202-206, 2006. doi: 10.1016/j.msea.2006.02.116.

boletim paranaense de Geociências
ISSN: 0067-964X

GU, C.; LIAN, J.; BAO, Y.; XIAO, W.; MUENSTERMANN, S. Numerical Study of the Effect of Inclusions on the Residual Stress Distribution in High-Strength Martensitic Steels During Cooling. Applied Sciences, v. 9, 455, 2019. doi: 10.3390/app9030455.

INTERNATIONAL ORGANIZATION FOR STANDARDIZATION. ISO 15510:2014 Stainless steels - Chemical composition, 2014.

LILLARD, R.; KA, M.; NIU, W. Pit Propagation at the Boundary between Manganese Sulfide Inclusions and Austenitic Stainless Steel 303 and the Role of Copper. Journal of The Electrochemical Society, v. 163, p. C440-C451, 2016. doi: 10.1149/2.0461608jes.

ŁAWRYNOWICZ, Z. Effect of The Degree of Cold Work and Sensitization Time on Intergranular Corrosion Behavior in Austenitic Stainless Steel. Advances in Materials Science, v. 19, p. 32-43, 2019. doi: 10.2478/adms-2019-0003.

MILAD, M.; ZREIBA, N.; ELHALOUANI, F.; BARADAI, C. The effect of cold work on structure and properties of AISI 304 stainless steel. Journal of Materials Processing Technology, v. 203, p. 80-85, 2008. doi: 10.1016/j.jmatprotec.2007.09.080.

MOEN, R. A.; DUNCAN, D. R. Cold work effects: a compilation of data for types 304 and 316 stainless steel. 1976. doi:10.2172/7180400.

MUTO, I.; IZUMIYAMA, Y.; HARA, N. Microelectrochemical Measurements of Dissolution of MnS Inclusions and Morphological Observation of Metastable and Stable Pitting on Stainless Steel. Journal of The Electrochemical Society, v. 154, 2007. doi: 10.1149/1.2745639.

NEWBY, J.; MILLS, K.; ASM HANDBOOK COMMITTEE. ASM Handbook, Vol. 9, Metallography and microstructures. ISBN 9-78087170-015-5, 1985.

OLIVEIRA, E. P.; MCNAUGHTON, N. J.; ARMSTRONG, R. Mesoarchaean to Palaeoproterozoic growth of the northern segment of the Itabuna-Salvador-Curaçá orogen, São Francisco craton, Brazil. Precambrian Research, v. 182, n. 1-2, p. 73-92, 2010.

PEDREIRA, A. J.; DE BRITO NEVES, B. B. Granites and associated rocks of the Bahia State, Brazil: a review. Lithos, v. 82, n. 3-4, p. 177-208, 2005.

PREFEITURA MUNICIPAL DE ITATIM, SECRETARIA MUNICIPAL DE EDUCAÇÃO, CULTURA, DESPORTO E LAZER. História do município de Itatim, 2020.

RAJA, V. S.; TETSUO, S. Stress corrosion cracking - Theory and practice. Cambridge: Woodhead Publishing, 2011.

SILVA, L. C.; FUCK, R. A. Geology of the São Francisco Craton. In: Geological Evolution of South America. Geological Society of America, p. 215-238, 2010.

SUTER, T.; BOHNI, H. Microelectrodes for corrosion studies in microsystems. Electrochimica Acta, v. 47, p. 191, 2001.

UIAA SAFETY COMMISSION, UNION INTERNATIONALE DES ASSOCIATIONS D'ALPINISME. UIAA 123: Rock Anchors 2020, 2021.

VUILLEMIN, B.; PHILIPPE, X.; OLTRA, R.; VIGNAL, V.; COUDREUSE, L.; DUFOUR, L.C.; FINOT, E. SVET, AFM and AES study of pitting corrosion initiated on MnS inclusions by microinjection. Corrosion Science, v. 45, p. 1143-1159, 2003. doi: 10.1016/S0010-938X(02)00222-6.

ACKNOWLEDGEMENTS

Special thanks are given to:

Departamento de Engenharia Mecânica da Universidade Tecnológica Federal do Paraná, DAMEC - UTFPR. Departamento Acadêmico de Tecnologia Mecânica da Universidade Federal da Bahia, DATM - UFBA and to the Instituto Laboratório de Análise de Minerais e Rochas da Universidade Federal do Paraná, iLAMIR - UFPR.

Submetido em 10/07/2024
Aceito em 26/07/2024
Editado por Inan Guilherme Senter (PET-GEOLOGIA/UFPR)